Inorg. Chem. **2007**, 46, 4177−4186

Inorganic Chemistry
Article

Three Novel Phases in the Sm–Co–Ga System. Syntheses, Crystal and Electronic Structures, and Electrical and Magnetic Properties

YongZhong Jia, Claude Belin,* Monique Tillard,* Laurence Lacroix-Orio, David Zitoun, and GuoHua Feng

Institut Charles Gerhardt, UMR 5253 CNRS UM2, AIME, Sciences et
Techniques du Languedoc, Université de Montpellier II, CC15, 2 Place Eugène Bataillon,
34095 Montpellier Cedex 5, France

Received January 16, 2007

This paper presents the synthesis, identification, and characterization of three novel phases in the ternary system Sm–Co–Ga: $SmCoGa_5$ (tP7, $HoCoGa_5$ type, tetragonal $P4/mmm$, $Z = 1$, $a = 4.2419(3)$ Å, and $c = 6.8559(5)$ Å), $Sm_4Co_3Ga_{16}$ (tP23, tetragonal $P4/mmm$, $Z = 1$, $a = 6.0620(5)$ Å, and $c = 11.1495(9)$ Å), and $SmCoGa_4$ (oC24, $YNiAl_4$ type, orthorhombic $Cmcm$, $Z = 4$, $a = 4.1246(6)$ Å, $b = 15.608(2)$ Å, and $c = 6.4556(9)$ Å). The structure of $SmCoGa_5$ was obtained from a multiphase X-ray powder Rietveld refinement whereas the crystal structures of the other two phases were determined from single-crystal X-ray analysis. Electronic structures were calculated for all phases by first-principles DFT methods. The atomic arrangements and bonding are discussed on the basis of the partial anionic networks involving Co and Ga atoms, and a strong structural correlation is observed between $SmCoGa_5$ and $Sm_4Co_3Ga_{16}$. The latter, which displays paramagnetic behavior, has a resistivity of 4.2 $\mu\Omega\cdot$cm at 3 K and undergoes a superconducting transition at 2.8 K.

Introduction

Recently, a new class of actinide-based superconductors has been discovered. The compound $PuCoGa_5$ displays a very high critical temperature $T_c = 18.5$ K that increases to 22 K under pressure.[1,2] It has been described with an unconventional antiferromagnetically mediated superconductivity,[3] but the superconducting mechanism is not completely elucidated and still raises debate.[4−9] Noteworthy is the phonon-mediated conventional superconductivity that occurs in the same temperature range, at 18 K for Nb_3Sn and 39 K for MgB_2. Attention was also paid to other potential actinide compounds of the $PuCoGa_5$ family that crystallize in the $HoCoGa_5$-type structure.[10] The physics and the chemistry of Ce-based intermetallic compounds have been extensively studied, and more than 200 papers were published last year. The $CeMIn_5$ (M = Co, Rh, Ir)[11,12] family is a special class among the heavy-fermion (HF) materials that has considerably advanced the knowledge of the interplay between superconductivity and magnetism.[3] These compounds, which show magnetic ordering and unconventional superconductivity at low temperatures,[13,14] are considered of great interest because they present the opportunity to study the competition or the coexistence of the two mechanisms.

---

* To whom correspondence should be addressed. E-mail: cbelin@univ-montp2.fr (C.B.), mtillard@univ-montp2.fr (M.T.). Fax: 33 04 67 14 33 04. Tel: 33 04 67 14 48 97.

(1) Sarrao, J. L.; Morales, L. A.; Thompson, J. D.; Scott, B. L.; Stewart, G. R.; Wastin, F.; Rebizant, J.; Boulet, P.; Colineau, E.; Lander, G. H. *Nature* **2002**, *420*, 297.

(2) Griveau, J. C.; Pfleiderer, C.; Boulet, P.; Rebizant, J.; Wastin, F. *J. Magn. Magn. Mater.* **2004**, *272*−*276*, 154,

(3) Curro, N. J.; Caldwell, T.; Bauer, E. D.; Morales, L. A.; Graf, M. J.; Bang, Y.; Balatsky, A. V.; Thompson, J. D.; Sarrao, J. L. *Nature* **2005**, *434*, 622.

(4) Maehira, T.; Hotta, T.; Ueda, K.; Hasegawa, A. *Phys. Rev. Lett.* **2003**, *90* (20), 207007.

(5) Soderlind, P. *Phys. Rev B: Condens. Matter Mater. Phys.* **2004**, *70*, 094515.

(6) Bang, Y.; Balatsky, A. V.; Wastin, F.; Thompson, J. D. *Phys. Rev.* **2004**, *70*, 104512.

(7) Raymond, S.; Piekarz, P.; Sanchez, J. P.; Serrano, J.; Krisch, M.; Janousova, B.; Rebizant, J.; Metoki, N.; Kanako, K.; Jochym, P. T.; Oles, A. M.; Parlinski, K. *Phys. Rev. Lett.* **2006**, *96*, 237003.

(8) Opahle, I.; Oppeneer, P. M. *Phys. Rev. Lett.* **2006**, *90*, 157001.

(9) Pourovskii, L. V.; Katsnelson, M. I.; Lichtenstein, A. I. *Phys. Rev. B: Condens. Matter Mater. Phys.* **2006**, *73*, 060506.

(10) Grin, Y. N.; Yarmolyuk, Y. P.; Gladishevsky, E. I. *Z. Kristallogr.* **1976**, *24*, 242.

(11) Moshopoulou, E. G.; Fisk, Z.; Sarrao, J. L.; Thompson, J. D. *J. Solid State Chem.* **2001**, *158*, 25.

(12) Macaluso, R. T.; Sarrao, J. L.; Pagliuso, P. G.; Moreno, N. O.; Goodrich, R. G.; Browne, D. A.; Fronczek, F. R.; Chan, J. Y. *J. Solid State Chem.* **2002**, *166*, 245.

(13) Petrovic, C.; Pagliuso, P. G.; Hundley, M. F.; Movshovich, R.; Sarrao, J. L.; Thompson, J. D.; Fisk, Z.; Monthoux, P. *J. Phys.: Condens. Matter* **2001**, *13*, L337.

10.1021/ic0700755 CCC: \$37.00

We were especially interested in focusing on the system Sm−Co−Ga and in searching for the compound $SmCoGa_5$. This work was motivated by the fact that Sm, with an electronic configuration and chemical properties close to those of Pu, is a much more accessible element. A look at the previous literature indicates that this Sm−Co−Ga ternary system is very complex since 18 phases have been reported from the Sm−Co−Ga phase diagram[15] and collected in the Pearson crystal structures handbook.[16]

Experimental Section

One incentive for the investigation of ternary phases with Sm and Co stems from the existence of numerous stable compounds: five in Sm−Ga and eight in Sm−Co binary systems whereas only one has been found in the Co−Ga system.[17] Although Ga has a very low melting point (303 K), a property which makes it an excellent medium for flux syntheses, alloying it with elements Sm and Co that melt respectively at 1345 and 1768 K requires high temperatures that are hardly affordable in classical furnaces. In arc-melting, a major problem is the weight loss in elements that have the lowest boiling points; this loss can be more or less reduced by properly adjusting the intensity of the electrode. Although many of our high-temperature furnace and arc-melting experiments have given nonhomogeneous products, we at last succeeded in preparing the hitherto unknown $SmCoGa_5$, $SmCoGa_4$, and $Sm_4Co_3Ga_{16}$ compounds and in determining their crystal structures.

As revealed by the X-ray powder pattern, a typical high-temperature (1373 K) alloying of the elements in the atomic ratio of 1:1:5 inside Ta tubes filled with Ar yielded a mixture of the binary compounds: $CoGa_3$, Co_5Sm, Co_3Sm, and Ga_3Sm_5. After that, the product was finely ground, pressed into a pellet, and then arc-melted. The resulting roundish ingot exhibited a few tiny single crystals on its surface, and they were characterized by energy-dispersive X-ray analysis (EDX) as $SmCoGa_4$ (Sm/Co/Ga ratio of 0.170(2)/0.165(2)/0.661(3); chemical standards are Co, GaAs, and $Sm_3Ga_5O_{12}$). The structure of the compound was determined from single-crystal X-ray intensity measurements.

The same reaction from the composition ratio of 1:1:5 was monitored in the classical furnace at the higher temperature of 1573 K and was then followed by slow cooling. The resulting product appeared fairly homogeneous and well crystallized; the powder pattern was indexed on the basis of one major component of $Sm_4Co_3Ga_{16}$ and small amounts of the side compounds of $SmGa_3$ and $CoGa_3$. The structure of $Sm_4Co_3Ga_{16}$ was also determined from single-crystal X-ray intensities, and it agrees with the chemical EDX analysis (Sm/Co/Ga ratio of 0.176(2)/0.137(2)/0.687(3)).

Regular-shaped crystals of $Sm_4Co_3Ga_{16}$ were chosen for electrical resistivity measurements using a standard four-probe method in the cryostat of a vibrating sample magnetometer (VSM) from Oxford Instruments, and measurements were performed in the range of 1.6−300 K with zero field under atmospheric pressure. Magnetic properties were measured using a superconducting quantum interference device magnetometer MPMS XL7, in a temperature range of 1.8−300 K and in a field range of 0−7 T. The temperature-dependent susceptibility was measured using the ac procedure. The sample was cooled to 1.8 K under zero magnetic field and measured from 1.8 to 300 K (zero-field cooled, ZFC). The field-cooled (FC) measurements were performed with an applied field during the cooling.

It was impossible to prepare $SmCoGa_5$ as a pure compound by the arc-melting of a mixture of the elements either taken strictly in the appropriate proportions or with an excess of Ga to compensate for its loss by evaporation. The other method used to prepare $SmCoGa_5$ consisted of alloying the binary compounds of $CoGa_3$ and $SmGa_3$. These had been first prepared from the elements in Ta tubes by high-temperature melting (note that in the Sm−Ga binary $SmGa_3$ represents a specific composition inside the single ϵ-hexagonal phase domain that ranges from $SmGa_4$ to $SmGa_2$).[18,19] Once prepared, the two binary products were finely ground, mixed intimately in a 1:1 proportion, pressed into a pellet, and then arc-melted. The resulting chunk appeared rather homogeneous under a microscope, but after it was broken into small pieces, no single-crystalline material could be isolated. The X-ray diffraction powder pattern lines were indexed on the basis of a large proportion (∼90%) of the compound $SmCoGa_5$, a small amount of $SmCoGa_4$, and a monoclinic impurity of unknown composition. The powder pattern was clear and precise enough to allow the Rietveld refinement of $SmCoGa_5$ in the same space group (*P*4/*mmm*) as that of $PuCoGa_5$.

X-ray Analysis. X-ray powder patterns were recorded on a Philips analytical X'pert diffractometer equipped with a Cu tube, a hybrid monochromator (parabolic multilayer mirror and two-crystal monochromator, Cu $K\alpha_{1,2}$ radiation, $\lambda = 1.5405$ and 1.5443 Å), and the Xcelerator detector.

Single crystals were selected under a microscope, placed at the tip of a glass fiber, and then mounted on the Xcalibur CCD (Oxford Diffraction) four-circle diffractometer for intensity measurements. The single-crystal structures were solved and refined with the programs *SHELXS 97*[20] and *SHELXL 97*,[21] and Rietveld analyses were carried out using the program *LHPM-Rietica*.[22] Single-crystal refinement data for $Sm_4Co_3Ga_{16}$ and $SmCoGa_4$ are collected in Table 1 whereas Tables 2−7 contain the fractional atomic positions, equivalent isotropic thermal displacement parameters, and selected bond distances for $SmCoGa_5$, $Sm_4Co_3Ga_{16}$, and $SmCoGa_4$.

Calculation Methods. DFT calculations of the electronic structures were performed using the gradient-corrected GGA-PW91 exchange and correlation functional[23] at the spin-unrestricted (polarized) level.

The program CASTEP[24] uses plane-wave basis sets to treat valence electrons and pseudopotentials to approximate the potential

---

(14) Petrovic, C.; Movshovich, R.; Jaime, M.; Pagliuso, P. G.; Hundley, M. F.; Sarrao, J. L.; Fisk, Z.; Thompson, J. D.; Monthoux, P. *Europhys. Lett.* **2001**, *53*, 354.

(15) Sichevich, O. M.; Grin, Y. N.; Yarmolyuk, Y. P. *Russ. Metall. Engl. Transl.* **1989**, *2*, 198.

(16) Villars, P.; Calvert, L. D. *Pearson's Handbook of Crystallographic Data for Intermetallic Phases*, 2nd ed.; ASM International: Materials Park, OH, 1991.

(17) Massalski, T. In *Binary Alloy Phase Diagrams*, 2nd ed.; Massalski, T. B., Okamoto, H., Subramanian, P. R., Kacprzak, L., Eds.; ASM International: Materials Park, OH, 1990.

(18) Yatsenko, S. P.; Semyannikov, A. A.; Semenov, G. B.; Chuntonov, K. A. *J. Less-Common Met.* **1979**, *64*, 185.

(19) Pelleg, J.; Kimmel, G.; Dayan, D. *J. Less-Common Met.* **1981**, *81*, 33.

(20) Sheldrick, G. M. *SHELXS 97*, A Program for Crystal Structure Determination; University of Göttingen: Göttingen, Germany, 1997.

(21) Sheldrick, G. M. *SHELXL 97*, A Program for Refining Crystal Structures; University of Göttingen: Göttingen, Germany, 1997.

(22) Hunter, B. A.; Howard C. J. *LHPM-Rietica: A Computer Program for Rietveld Analysis of X-ray and Neutron Powder Diffraction Patterns*, version 1.7.7; ANSBTO, Lucas Heights Research Laboratories: Menai, Australia, 1998.

(23) Perdew, J. P.; Chevary, J. A.; Vosko, S. H.; Jackson, K. A.; Pederson, M. R.; Singh, D. J.; Fiolhais, C. *Phys. Rev. B*: *Condens. Matter Mater. Phys.* **1992**, *46*, 6671.

(24) Payne, M. C.; Teter, M. P.; Allan, D. C.; Arias, T. A.; Joannopoulos, J. D. *Rev. Mod. Phys.* **1992**, *64, 1045.* CASTEP is distributed inside the commercial pack: Materials Studio version 3.1.0; Accelrys, Inc.: San Diego, 2004.

Table 1. Crystallographic Refinement Data for $Sm_4Co_3Ga_{16}$ and $SmCoGa_4$

empirical formula	$Sm_4Co_3Ga_{16}$	$SmCoGa_4$
fw	473.43	488.17
cryst syst	tetragonal	orthorhombic
space group	*P*4/*mmm*	*Cmcm*
unit cell dimens (Å)	$a = 6.0620(5)$ $b = 6.0620(5)$ $c = 11.1495(9)$	$a = 4.1246(6)$ $b = 15.608(2)$ $c = 6.4556(9)$
V (Å^3)	409.72(6)	415.6(1)
Z	1	4
density	7.675	7.802
abs coeff (mm^{-1})	42.768	43.129
F(000)	825	851
cryst size (mm^3)	0.25 × 0.14 × 0.06	0.14 × 0.09 × 0.08
θ range for data collection (deg)	3.36−32.32	4.10−32.24
reflns collected	6873	3511
independent reflns	474 [R(int) = 0.0441]	423 [R(int) = 0.0432]
completeness (%)	96.1	95.1
refinement method	full matrix least squares on F^2	
data/restraints/params	474/0/28	423/0/24
GOF on F^2	1.328	1.203
final indices [$I > 2\sigma(I)$][a]	0.0262 0.0626	0.0269 0.0562
indices (all data)	0.0273 0.0630	0.0352 0.0580
largest diff peak and hole (e·Å^{-3})	2.017/−2.011	1.891/-1.939

[a] $R1 = \Sigma(|F_o| - |F_c|)/\Sigma|F_o|$, $wR2 = [\Sigma[w(F_o^2 - F_c^2)]/[\Sigma w|F_o|^2)^2]^{1/2}$.

field of ion cores. We used the ultrasoft pseudopotentials (USPPs) generated for each element according to the Vanderbilt[25] scheme, which allows calculations to be performed at a lower energy cutoff than when norm-conserving pseudopotentials are used. As usual for transition elements, a partial core-corrected USPP was used for Co. Since high-lying shallow-core Sm 5s and 5p orbitals may hybridize with 5d and 4f orbitals, ultrasoft pseudopotentials treat them as valence states. The inner 3d levels of Ga were also considered as valence states. The kinetic cutoff energies were set at 330 or 380 eV (medium or fine quality). We used a density-mixing scheme[26] and a Monkhorst-Pack uniform grid[27] of automatically generated *k* points; in any case, the spacing between the grid points in reciprocal space was taken at less than 0.05 Å^{-1}.

The program DMOL^3 [28] uses numerical basis sets (DND, double numerical and a polarization d function). For Sm, the $5s^25p^64f^66s^2$ electrons were treated as valence electrons and core electrons were replaced by a density functional semicore pseudopotential that introduces some degree of relativistic effect. Single effective potentials were also used for Co and Ga atoms.

The ADF-BAND program[29] uses numerical atomic orbitals in addition to Slater-type orbitals to get an even better description with only a limited number of basis functions. Double-ζ functions were used for Co and Ga whereas a triple-ζ basis set augmented with two polarization functions was used for Sm. Scalar relativistic effects were taken into account with the zero-order regular approximation method.

Results and Discussion

Structural Comparison of Compounds $SmCoGa_5$ and $Sm_4Co_3Ga_{16}$. $SmCoGa_5$. Despite the presence, as impurities in the product, of $SmCoGa_4$ described below and an incompletely characterized monoclinic phase ($a = 7.822$ Å, $b = 7.051$ Å, $c = 6.169$ Å, $\beta = 99.08°$), a three-phase Rietveld refinement of the experimental X-ray powder pattern (Figure 1) was successfully achieved for $SmCoGa_5$ (of $HoCoGa_5$ type) in the tetragonal space group *P*4/*mmm* ($R_p = 1.36\%$, $R_{wp} = 2.03\%$, $R_{Bragg} = 4.64\%$, GOF = 3.35). The refined unit cell parameters, $a = 4.2419(3)$ Å and $c = 6.8559(5)$ Å, are on the order of those reported for the isostructural compounds $RCoGa_5$ (R = Y, Gd−Tm, Lu, Pu).[1,10,30] The specific internal Ga1 *z* coordinate converged to 0.303 and is consistent with the value of 0.312 reported for the isostructural $PuCoGa_5$ compound ($a = 4.232$ Å and $c = 6.786$ Å).

In this structure (Figure 2), the Ga1 atoms are disposed at the vertices of a flattened cube of which the face (001) is capped by the Ga2 atom and the face parallel to (110) is capped by a Co atom. The three-dimensional (3D) network is built essentially through short Co1−Ga1 (2.5142 Å) and relatively long Ga1−Ga2 (2.969 Å) bonds. The Sm atom, 8-fold coordinated (2.969 Å) to Ga1 and 4-fold coordinated (2.999 Å) to Ga2, sits at the center of a quasi-regular cuboctahedron of Ga.

The isostructural compound $CeCoIn_5$ was described on the basis of such cuboctahedra[11] that constitute also the cubic 3D $CeIn_3$ compound ($AuCu_3$-type structure[31]). The cuboctahedra that contain the f elements are fused to each other by sharing faces to form a two-dimensional (2D) network [$CeIn_3$] parallel to the *ab* plane while the layer [$CoIn_2$] forms parallelepipeds sharing edges and fused to the $CeIn_3$ layer through square faces.

$Sm_4Co_3Ga_{16}$. The tetragonal structure of $Sm_4Co_3Ga_{16}$ (Figure 3) was solved using X-ray single-crystal data, in space group *P*4/*mmm*, with $a = 6.0620(5)$ Å and $c = 11.1495(9)$ Å, and refined to R1 (wR2) = 2.62 (6.26)%, GOF = 1.33. At first sight, there is a strong correlation between the tetragonal *P*4/*mmm* structures of $SmCoGa_5$, $Sm_4Co_3Ga_{16}$, and the one of Sm_2CoGa_8 represented in Figure 4. Work on the series R_2CoGa_8 (R = Sm, Gd, Tb, Dy, Ho, Er, Tm, Lu, Y) was reported 3 decades ago. The structure of Ho_2CoGa_8 was determined from a single crystal on the basis of 122 reflection intensities collected by the Weissenberg technique (*P*4/*mmm*, $a = 4.217$ Å and $c = 10.97$ Å, $R(F) = 0.139$). This structure is now referred to as the Ho_2CoGa_8-type structure to which Sm_2CoGa_8[10] ($a = 4.264$ Å and $c = 11.14$ Å, with no further structural determination to our knowledge) has been claimed to belong.[10]

$Sm_4Co_3Ga_{16}$, in which the entire crystal structure of $SmCoGa_5$ can be recognized in the range of *z* values from ca. 0.2 to 0.8, can be described as already done for the $RMIn_5$

---

(25) Vanderbilt, D. *Phys. Rev.* **1990**, *B41*, 7892−7895.
(26) Kresse, G.; Furthmuller, J. *Phys. Rev.* **1996,** *B54*, 11169−11186.
(27) Monkhorst, H. J.; Pack, J. D. *Phys. Rev.* **1977**, *B16*, 1748.
(28) (a) Delley, B. *J. Chem. Phys.* **1990**, *92*, 508. (b) Delley, B. *Int. J. Quantum Chem.* **1998**, *69*, 423. (c) Delley, B. *J. Phys. Chem.* **1996**, *100*, 6107. DMOL^3 is distributed inside the commercial pack: Materials Studio version 3.1.0; Accelrys, Inc.: San Diego, 2004.
(29) te Velde, G.; Baerends, E. J.; Philipsen, P. H. T.; Wiesenekker, G.; Groeneveld, J. A.; Kootstra, F.; de Boeij, P. L.; Snijders J. G. BAND2004.01; SCM, Theoretical Chemistry, Vrije Universiteit: Amsterdam, The Netherlands. http://www.scm.com.
(30) Hudis, J.; Hu, R.; Broholm, C. L.; Mitrovic, V. F.; Petrovic, C. *J. Magn. Magn. Mater.* **2006**, *307*, 301.
(31) Knebel, G.; Braithwaite, D.; Canfield, P. C.; Lapertot, G.; Flouquet, J. *Phys. Rev.* **2001**, *B65*, 24425.

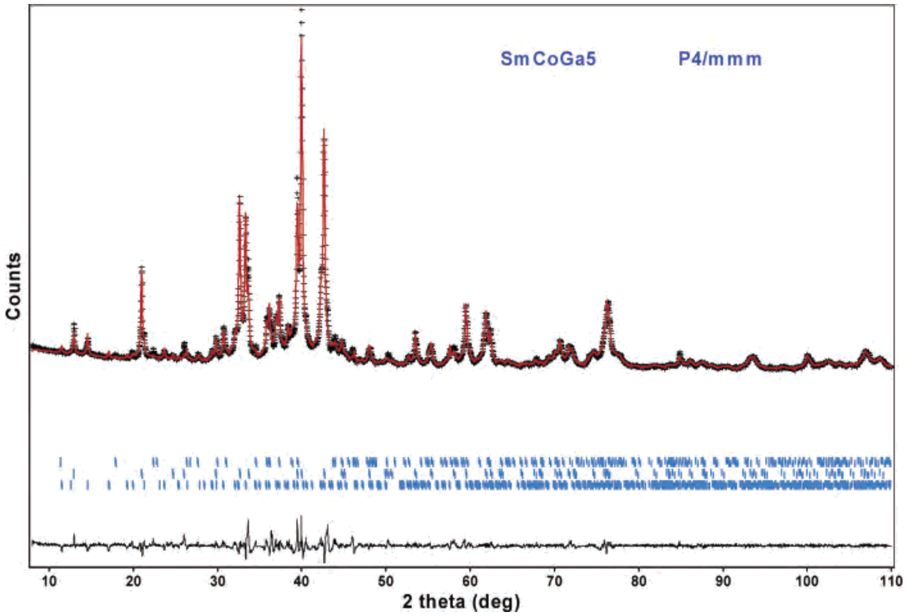

Figure 1. Observed (data points), calculated (solid line), and difference (bottom) room-temperature X-ray diffraction powder patterns (Cu K$\alpha_{1,2}$, λ = 1.5405 and 1.5443 Å) for an alloy prepared by arc-melting of a $SmGa_3$/$CoGa_3$ mixture, resulting preponderantly (90%) in $SmCoGa_5$.

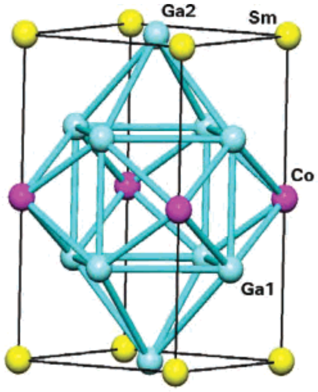

Figure 2. Representation of the $SmCoGa_5$ unit cell (a = 4.2419 Å and c = 6.8559 Å, tetragonal space group $P4/mmm$). Ga−Ga contacts have been drawn up to 3 Å.

Table 2. Atomic Positional and Isotropic Displacement Parameters in the Tetragonal ($P4/mmm$) Compound $SmCoGa_5$

atom	Wyckoff site	x	y	z	U_{iso} (Å^2)
Sm	1a	0	0	0	0.027(1)
Co1	1b	0	0	$^1/_2$	0.024(2)
Ga1	4i	0	$^1/_2$	0.3030(2)	0.044(6)
Ga2	1c	$^1/_2$	$^1/_2$	0	0.072(2)

Table 3. Selected Interatomic Distances (Å) and Atom Coordinations in $SmCoGa_5$

Co1	8 × Ga1	2.5142(9)	Ga1	2 × Co1	2.5142(9)
Sm	8 × Ga1	2.969(1)	Ga1	2 × Sm	2.969(1)
Sm	4 × Ga2	2.9995(1)	Ga2	4 × Sm	2.9995(1)
Ga1	Ga1	2.701(2)	Ga1	2 × Ga2	2.969(1)
Ga1	4 × Ga1	2.9995(1)			

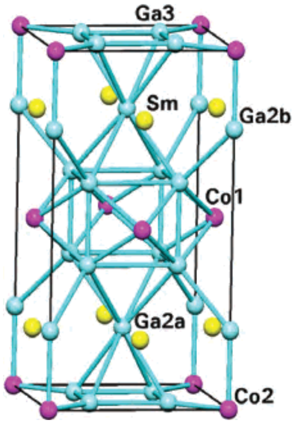

Figure 3. Representation of the $Sm_4Co_3Ga_{16}$ unit cell (a = 6.0620 Å and c = 11.1495 Å, tetragonal space group $P4/mmm$). Note that atoms have been labeled for comparison with $SmCoGa_5$.

Table 4. Atomic Coordinates and Equivalent Displacement Parameters in the Tetragonal ($P4/mmm$) Compound $Sm_4Co_3Ga_{16}$

atom	Wyckoff site	x	y	z	U_{eq} (Å^2)^a
Sm	4i	0	$^1/_2$	0.19458(4)	0.0079(2)
Co1	2e	0	$^1/_2$	$^1/_2$	0.0075(3)
Co2	1a	0	0	0	0.0109(5)
Ga1	8r	0.24972(8)	0.24972(8)	0.38553(7)	0.0112(2)
Ga2a	2h	$^1/_2$	$^1/_2$	0.1953(1)	0.0113(3)
Ga2b	2g	0	0	0.2199(2)	0.0109(3)
Ga3	4j	0.2813(1)	0.2813(1)	0	0.0105(2)

[a] U_{eq} is defined as one-third of the trace of the orthogonalized U_{ij} tensor.

and R_2MIn_8 families (R = rare-earth elements)[32] on the basis of the sequential stacking of $AuCu_3$- and $PtHg_2$-type fragments. As shown in Figure 4, the difference between R_2CoGa_8 and $Sm_4Co_3Ga_{16}$ results from the presence of a Co atom inside the [$SmGa_3$] layer. A superstructure (a = 6.062 Å and c = 11.149 Å) is then built from Sm_2CoGa_8 (a = 4.264 Å and c = 11.14 Å) by filling with one Co atom over two squares of Ga within the ab plane (Figure 4, middle, top). The arising of the Co−Ga bond (2.412 Å) induces the shortening of the Ga3−Ga3 distance from 3.015 to 2.651 Å. To go back to the comparison with $SmCoGa_5$, within the plane containing Sm, the Ga2 atom (in $SmCoGa_5$) has given place to Ga2a and Ga2b in $Sm_4Co_3Ga_{16}$ (Figure 3), and

---

(32) Pagliuso, P. G.; Thompson, J. D.; Hundley, M. F.; Sarrao, J. L.; Fisk, Z. *Phys. Rev. B: Condens. Matter Mater. Phys.* **2001**, *63*, 054426.

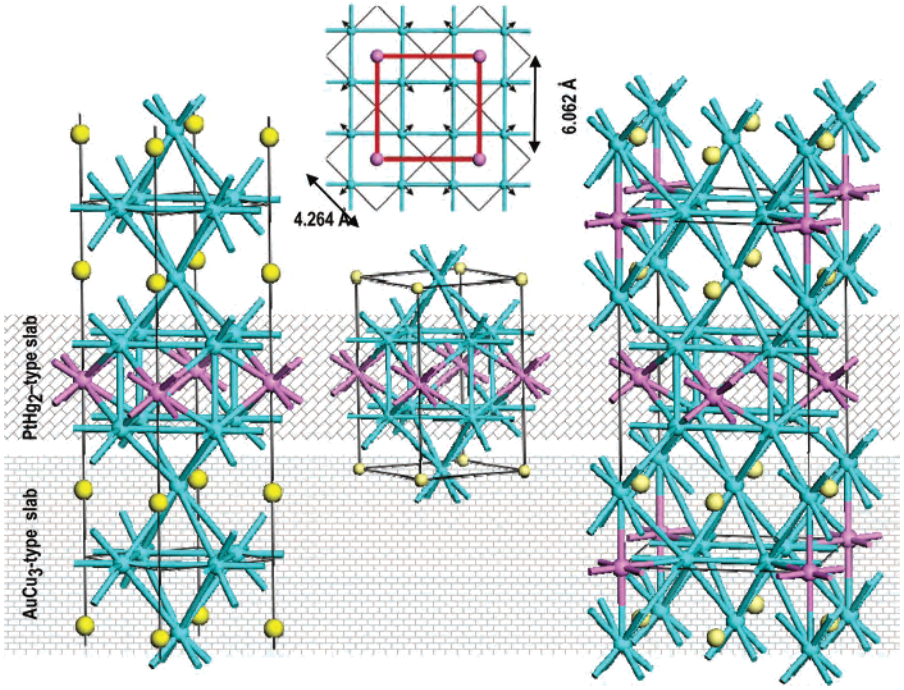

Figure 4. Representation of the tetragonal *P*4/*mmm* structures of Sm_2CoGa_8 (left), $SmCoGa_5$ (middle, bottom), and $Sm_4Co_3Ga_{16}$ (right). The difference between $Sm_4Co_3Ga_{16}$ ($a = 6.062$ Å and $c = 11.149$ Å) and Sm_2CoGa_8 ($a = 4.264$ Å and $c = 11.14$ Å) arises from the presence of one additional Co atom in the square base of the $AuCu_3$-type layer. A superstructure is then built (middle, top) by filling one Co atom over two squares of Ga, which induces the shortening of the Ga−Ga distance from 3.015 to 2.651 Å.

Table 5. Interatomic Distances (Å) and Atom Coordinations in $Sm_4Co_3Ga_{16}$

Co1	8 × Ga1	2.4945(4)	Co2	4 × Ga3	2.412(1)
Sm	4 × Ga1	3.0209(6)	Co2	2 × Ga2b	2.451(2)
Sm	2 × Ga2a	3.0310(3)	Ga1	2 × Co1	2.4945(4)
Sm	2 × Ga2b	3.0441(3)	Ga1	Ga1	2.553(2)
Sm	4 × Ga3	3.0614(4)	Ga1	Ga2b	2.828(1)
Ga2a	4 × Ga3	2.874(1)	Ga1	2 × Sm	3.0209(6)
Ga2a	4 × Sm	3.031(5)	Ga3	Co2	2.412(1)
Ga2b	Co2	2.452(2)	Ga3	2 × Ga3	2.651(2)
Ga2b	4 × Ga1	2.828(1)	Ga3	2 × Ga2a	2.874(1)
Ga2b	4 × Sm	3.0441(3)	Ga3	4 × Sm	3.0614(4)

subsequently, the unique long distance of 2.969 Å between Ga1 and Ga2 ($SmCoGa_5$) is split into 3.017 Å (Ga1−Ga2a) and 2.828 Å (Ga1−Ga2b).

The comparative analysis of the interatomic distances is informative on the nature and localization of bonding within these compounds. In all structures, Sm is surrounded by 12 Ga atoms: eight at 2.969 Å and four at 2.999 Å in $SmCoGa_5$ and eight at 3.007 Å and four at 3.020 Å in Sm_2CoGa_8 instead of four at 3.021 Å, two at 3.031 Å, two at 3.044 Å, and four at 3.061 Å in $Sm_4Co_3Ga_{16}$.

The shortest interatomic distances involve the eight-coordinated Co atom, and the Co−Ga length is 2.514 Å in $SmCoGa_5$, 2.510 Å in Sm_2CoGa_8, and 2.495 Å in $Sm_4Co_3Ga_{16}$. In the latter, the additional Co atom (Co2) is coordinated to six Ga atoms: four Ga3 at 2.412 Å and two Ga2b at 2.451 Å. In these structures, there are only a few short contacts between Ga atoms along the ⟨001⟩ direction, and the Ga1−Ga1 length of 2.701 Å in $SmCoGa_5$ is shortened to 2.649 Å in Sm_2CoGa_8 and to 2.553 Å in $Sm_4Co_3Ga_{16}$.

With regard to Sm_2CoGa_8, this superstructure gives some good small statistical intensity reflections, having $h + k$ with an odd value, and its simulated powder pattern (Cu Kα) represented in Figure 5 is indexed in the two *P*4/*mmm* cells ($a = 4.264$ Å and $c = 11.14$ Å; $a = 6.062$ Å and $c = 11.149$ Å).

Crystal Structure of $SmCoGa_4$. The crystal structure of $SmCoGa_4$ was solved in the orthorhombic space group *Cmcm*, with $a = 4.1246(6)$ Å, $b = 15.608(2)$ Å, and $c = 6.4556(9)$ Å, and refined from X-ray single-crystal intensities to R1 (wR2) = 2.69 (5.62)%, GOF = 1.20. This compound belongs to the $YNiAl_4$ type and is isostructural with $SmNiGa_4$[33] and $YbNiGa_4$.[34]

As shown in Figure 6, the 3D network of $SmCoGa_4$ may be described with alternate slabs: a nearly square 2D network of Ga2 and Ga3, puckered by folding along the Ga2−Ga2 square diagonal, and a corrugated 2D slab of Ga1 rings (boat conformation) filled with Co atoms. These slabs, stacked along the *b* axis, are interconnected through very short Co−Ga2 bonds (2.308 Å). The Sm atom lies within a 17-atom cavity (4 Co and 13 Ga atoms). These cavities are fused to each other through the sharing of 5-atom rings, forming channels parallel to the *a* axis.

Electronic Structure Calculations and Properties. As indicated by the electrical resistivity and magnetic measurements on $Sm_4Co_3Ga_{16}$, all these ternary materials would be expected to exhibit some metallic properties and magnetic moments. According to the Pauling electronegativities ($\chi =$ 1.2, 1.6, and 1.8 for Sm, Ga, and Co, respectively), we might reasonably assign the formal charge 3+ to Sm whereas Co should be the most reduced element in the alloys. To gain

---

[33] Romaka, V. A.; Grin, Yu.; Yarmoluk, Ya.P. *Ukr. Fiz. Zh.* **1983**, *28* (7), 1095.

[34] Vasylechko, L.; Schnelle, W.; Schmidt, M.; Burkhardt, U.; Borrmann, H.; Schwarz, U.; Grin, Yu. *J. Alloys Compd.* **2006**, *416*, 35.

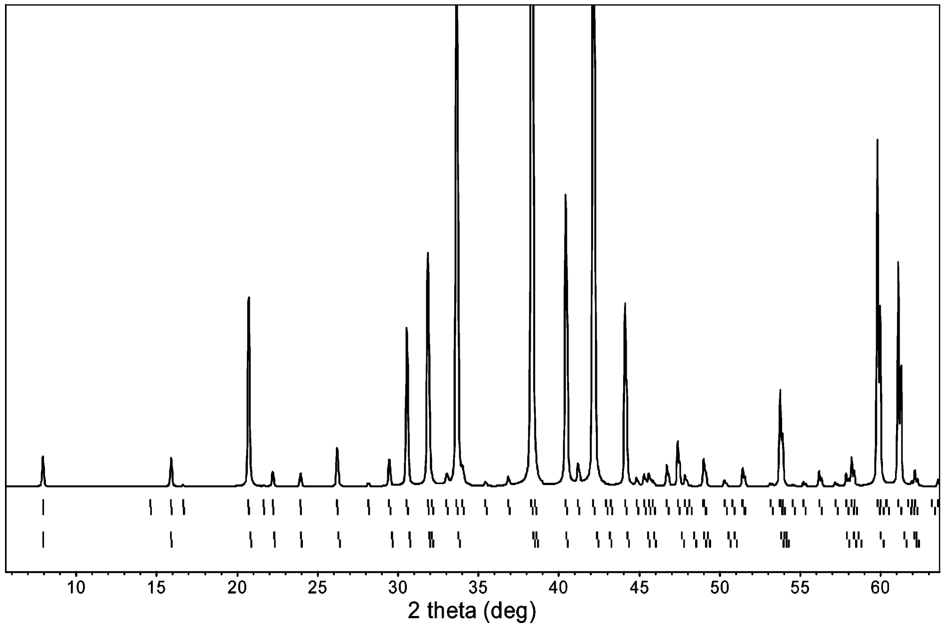

Figure 5. Representation of the simulated X-ray powder pattern calculated for $Sm_4Co_3Ga_{16}$ (Cu K$\alpha_{1,2}$). The lines are indexed in the tetragonal *P*4/*mmm* unit cells: $a = 6.062$ Å and $c = 11.149$ Å for $Sm_4Co_3Ga_{16}$ (upper ticks) and $a = 4.264$ Å and $c = 11.14$ Å for Sm_2CoGa_8 (lower ticks).

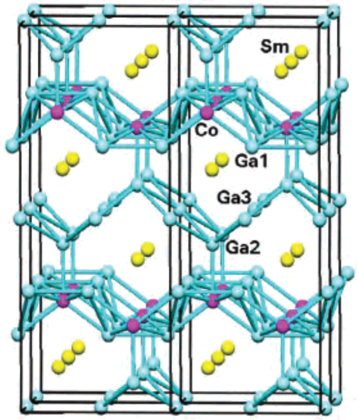

Figure 6. Packing within the orthorhombic structure of $SmCoGa_4$ (*Cmcm*, $a = 4.1246$ Å, $b = 15.608$ Å, and $c = 6.4556$ Å) approximately viewed along the *a* axis. For clarity, only the atomic contacts less than 2.90 Å are drawn.

Table 6. Atomic Coordinates and Equivalent Displacement Parameters in $SmCoGa_4$ (Orthorhombic *Cmcm*)

atom	Wyckoff site	*x*	*y*	*z*	U_{eq} (Å^2)
Sm	4*c*	0	0.88343(4)	$^1/_4$	0.0085(2)
Co	4*c*	0	0.2242(1)	$^1/_4$	0.0140(4)
Ga1	8*f*	0	0.31164(6)	−0.0512(1)	0.0107(2)
Ga2	4*c*	0	0.07626(9)	$^1/_4$	0.0135(3)
Ga3	4*a*	$^1/_2$	0	0	0.0128(3)

Table 7. Interatomic Distances (Å) and Atom Coordinations in $SmCoGa_4$

Sm	Ga2	3.010(1)	Sm	4 × Ga1	3.0480(7)
Sm	4 × Ga3	3.1888(4)	Sm	2 × Co	3.230(1)
Sm	Ga2	3.2889(6)	Co	Ga2	2.308(2)
Co	4 × Ga1	2.4923(7)	Co	2 × Sm	3.230(1)
Ga1	Co	2.376(1)	Ga1	2 × Co	2.4923(7)
Ga1	Ga1	2.566(2)	Ga1	2 × Ga1	2.897(1)
Ga1	2 x Sm	3.0480(7)	Ga1	Sm	3.304(1)
Ga2	Co	2.308(2)	Ga2	4 × Ga3	2.8765(6)
Ga2	Sm	3.010(1)	Ga2	2 × Sm	3.2886(5)
Ga3	4 × Ga2	2.8765(6)	Ga3	4 × Sm	3.1888(4)

some insight into the understanding of these phases and bonding therein, we have calculated the electronic structures for the three compounds.

First-principles calculations relative to the lanthanide and actinide compounds have been widely discussed. In the systems containing f elements, strong electron correlations cannot be correctly described in the framework of the conventional DFT-LDA (LDA = local density approximation) theory. Such treatment may lead to erroneous electronic properties, for example, as in the case of UO_2, which was found to be metallic instead of insulating. However, good results may be obtained using GGA gradient-corrected functionals in cases where spin−orbit interactions have little influence on the structural properties.[35] To calculate accurate structural energies,[36] relativistic effects have to be included in the calculations.

$SmCoGa_5$. Among the three compounds studied in this work, $SmCoGa_5$, with only seven atoms in its unit cell, is the most computationally affordable at the ab initio level.

A geometry optimization was first performed with CASTEP (*P*4/*mmm* symmetry-constrained, BFGS algorithm) by simultaneously varying the cell parameters and the *z* internal coordinate of the Ga1 atom. Results from spin-unrestricted and spin-restricted calculations are compared in Table 8.

Calculated lattice constants deviate from the experimental values by less than 1.8%, and the *z* coordinate of Ga1 deviates by less than 3.8%. This looks good with regard to the structural parameters obtained from a multiphase powder refinement. However, the lattice parameters of $SmCoGa_5$ from the unrestricted calculation are in poorer agreement with the experiment than those from the spin-restricted one. This

---

(35) Pickard, C.; Winkler, B.; Chen, R. K.; Payne, M. C.; Lee, M. H.; Lin, J. S.; White, J. A.; Milman, V.; Vanderbilt, D. *Phys. Rev. Lett.* **2000**, *85* (24), 5122.

(36) Soderlind, P. *Adv. Phys.* **1998**, *47*, 959.

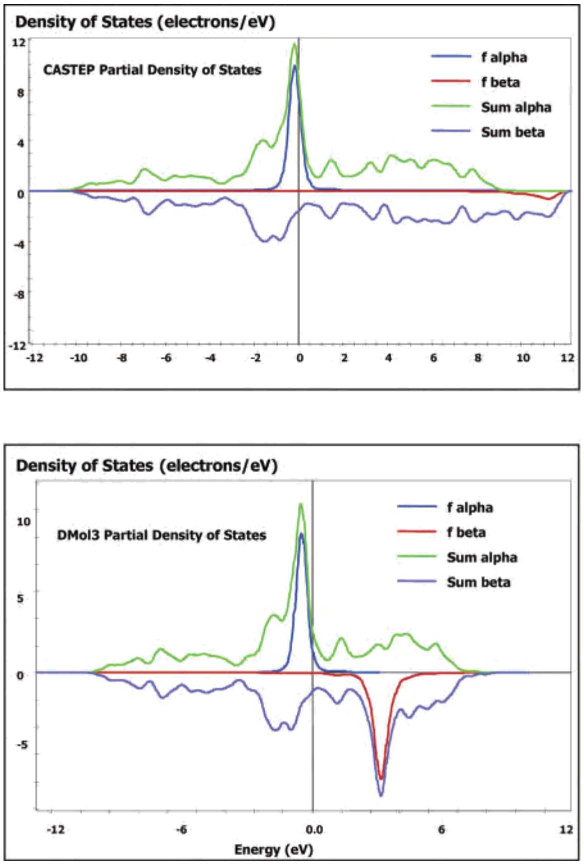

Figure 7. Representation of partially polarized DOS for compound $SmCoGa_5$ calculated with CASTEP (top) and DMOL^3 (bottom). In the nonrelativistic calculation (CASTEP), the Sm 4f levels are pinned at the Fermi level with only spin-up density (spin charge 6.12). Scalar relativistic effects are introduced in the DMOL^3 calculation (spin charge 5.806).

Table 8. Comparison of Experimentally Determined (Room Temperature) and CASTEP DFT Optimized Parameters of $SmCoGa_5$ in Spin-Restricted and Spin-Unrestricted Configurations

		experimental	spin-restricted	unrestricted
a (Å)		4.2419	4.2648 (+0.5%)	4.2888 (+1.1%)
c (Å)		6.8559	6.8921 (+0.5%)	6.9799 (+1.8%)
Ga1(*z*)		0.3030	0.3102 (+2.3%)	0.3145 (+3.8%)
total energy (eV)			−13514.49	−13530.11
spin (ℏ)	Sm			3.13
	Co			−0.02
	Ga1/Ga2			0.01/-0.01
charge	Sm		0.09	0.25
	Co		−0.56	−0.59
	Ga1/Ga2		−0.06/+0.13	0.03/0.08

might stem from the failure of the local spin density approximation, generalized gradient approximation (LSDA-GGA) to treat correctly the strongly correlated systems with localized 4f states (narrow bandwidth) at E_F. However, this discrepancy due to the strong on-site Coulomb repulsion among the 4f electrons might be corrected with the DFT+U method in which a Hubbard-like term is added to the DFT Hamiltonian.[37]

The calculated electronic densities of states (DOS) indicate that $SmCoGa_5$ is likely to display some metallic character (Figure 7), and the total energy has been found to be 2.23 eV/atom lower for the unrestricted (spin-polarized) configuration.

Table 9. Mulliken Atomic and Spin Charges Calculated with CASTEP, DMOL^3, and ADF-BAND for the Compound $SmCoGa_5$

	CASTEP		DMOL^3		ADF-BAND	
	atomic charge	spin charge	atomic charge	spin charge	atomic charge	spin charge
Sm	0.340	6.200	2.506	5.806	2.358	5.545
Ga1	0.050	−0.020	−0.295	0.009	−0.338	0.006
Ga2a	−0.140	−0.040	−0.649	0.001	−0.555	0.003
Co1	−0.390	−0.140	−0.675	−0.090	−0.451	0.009

The Mulliken atomic and spin charges obtained with the CASTEP, DMOL^3, and ADF-BAND calculations are reported for $SmCoGa_5$ in Table 9. Note that the CASTEP atomic charges are fairly different from those obtained with DMOL^3 and ADF-BAND. In fact, the Mulliken charges and bond populations are calculated in CASTEP following the formalism described by Segall et al.[38,39] Due to the delocalized nature of the basis states, plane waves do not give information regarding the localization of the electrons in the system; in contrast, the use of linear combination of atomic orbitals (LCAO) basis sets provides a natural way of specifying atomic charges and bond populations. In CASTEP, population analysis is performed using a projection of the plane-wave states onto a localized basis,[40] to which the Mulliken formalism[41] is then applied. On the other hand, DMOL^3 and ADF-BAND, which incorporate relativistic effects, together yield very comparable band structures, DOS, spins, and atomic charges. As a consequence, the Sm 4f orbitals which are found pinned at the Fermi level in the nonrelativistic CASTEP calculation are split on both sides of E_F when using ADF-BAND and DMOL^3 (Figure 7).

$Sm_4Co_3Ga_{16}$. The band structure and DOS are comparatively represented for the two compounds $Sm_4Co_3Ga_{16}$ and $SmCoGa_5$ (Figure 8). These electronic structures are clearly different, emphasizing the more 2D nature in conduction properties for $SmCoGa_5$ (weak dispersion with no band crossing the Fermi level along the [001] direction). The electronic properties look more isotropic for $Sm_4Co_3Ga_{16}$ which, with a higher DOS at the Fermi level, appears more metallic than $SmCoGa_5$. Actually, as indicated by the Mulliken atomic charges given in Table 10, in $Sm_4Co_3Ga_{16}$ the positive charge on Sm is less than that in $SmCoGa_5$ and the anionic charge is more evenly distributed over the Ga atoms. For both compounds, within the energy range of ∼3 eV (∼0.1 hartree) below E_F, the DOS are mainly governed by overlapping Co 3d and Ga 4p orbitals whereas the little dispersed Sm 4f orbital remains practically inert.

The electron-density differences calculated with CASTEP for $SmCoGa_5$ and $Sm_4Co_3Ga_{16}$ provide a good overview of the electronic charge redistribution due to some interatomic bonding in the system (Figure 9). In $SmCoGa_5$, 2D-like bonding within a layer perpendicular to the *c* axis involves the atoms Co1 and Ga1. There is no apparent electron

---

(37) Petersen, M.; Hafner, J.; Marsman, M. *J. Phys.: Condens. Matter* **2006**, *18*, 7021.

(38) Segall, M. D.; Pickard, C. J.; Shah, R.; Payne, M. C. *Mol. Phys.* **1996**, *89*, 571.

(39) Segall, M. D.; Shah, R.; Pickard, C. J.; Payne, M. C. *Phys. Rev.* **1996**, *B54*, 16317.

(40) Sanchez-Portal, D.; Artacho, E.; Soler, J. M. *Solid State Commun.* **1995**, *95*, 685.

(41) Mulliken, R. S. *J. Chem. Phys.* **1955**, *23*, 1833.

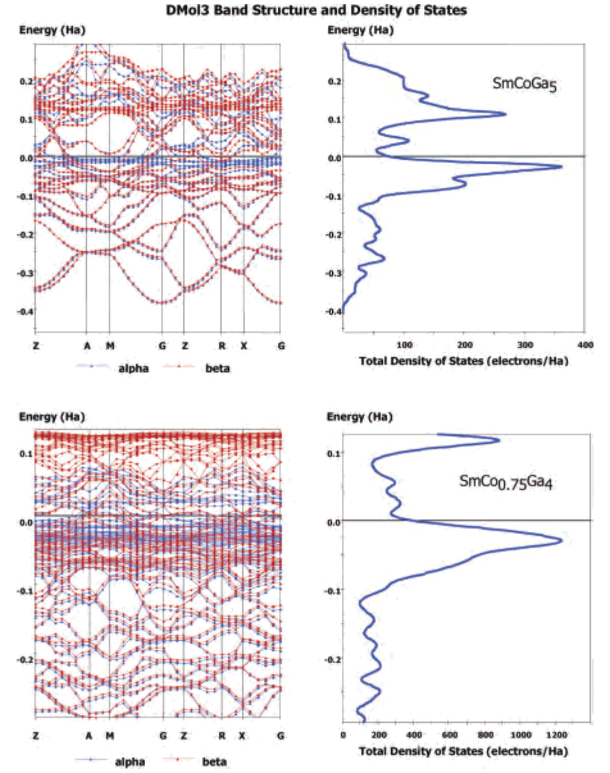

Figure 8. Representation of band structures and total DOS calculated with DMOL^3 for compounds $SmCoGa_5$ and $Sm_4Co_3Ga_{16}$.

Table 10. Compared Mulliken Atomic and Spin Charges (DMOL^3 and GGA-PW91)

	$SmCoGa_5$		$Sm_4Co_3Ga_{16}$		$SmCoGa_4$	
atom	atomic charge	spin charge	atomic charge	spin charge	atomic charge	spin charge
Sm	2.506	5.806	1.970	5.810	2.678	5.830
Ga1	−0.295	0.009	−0.216	−0.008	−0.442	0.013
Ga2a	−0.649	0.001	−0.489	0.010	−0.518	0.005
Co1	−0.675	−0.090	−0.678	−0.070	0.176	1.437
Ga2b			−0.518	0.005		
Ga3			−0.492	0.015	−0.549	−0.009
Co2			−0.816	0.065		

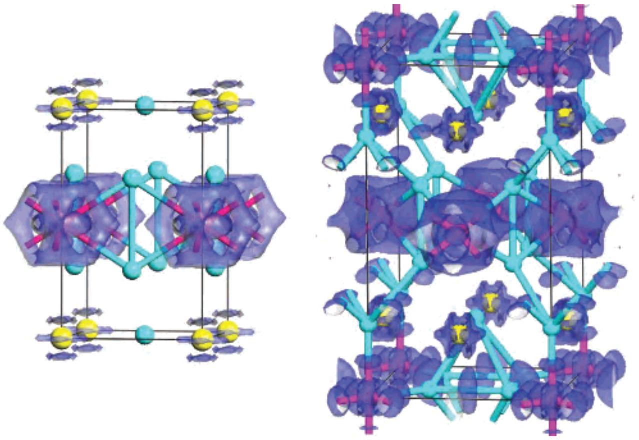

Figure 9. Representation of the electron-density difference (isovalue level 0.032 e·Å^{-3}) in the $SmCoGa_5$ (left) and $Sm_4Co_3Ga_{16}$ (right) compounds. The electron-density difference is obtained by subtracting the isolated atom densities from the overall electron density.

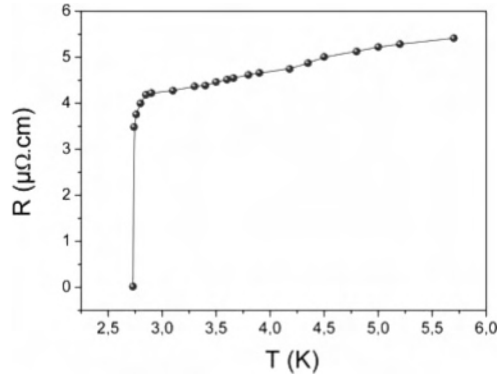

Figure 10. Electrical resistivity measurements for compound $Sm_4Co_3Ga_{16}$ using a four-probe method. The results are shown only for temperatures below 6 K.

density that bounds Ga2, the more reduced Ga atom, to neighboring Ga atoms. Also, at the isovalue level of 0.032 e·Å^{-3}, no density is visible around Sm, featuring its cationic nature. For compound $Sm_4Co_3Ga_{16}$, bonding at the middle layer (Co1−Ga1) looks like that in $SmCoGa_5$; in addition, there is consistent bonding within the basal layers (Co2−Ga3 and Ga3−Ga3). On the other hand, there is some weak bonding between these layers involving the Co2, Ga2b, and Ga1 atoms that provides the structure with some degree of three-dimensionality.

Electrical and Magnetic Properties of $Sm_4Co_3Ga_{16}$. $Sm_4Co_3Ga_{16}$ is the only compound that could be prepared pure, and the results from the electrical and magnetic measurements follow. $Sm_4Co_3Ga_{16}$ presents a resistivity of 4.2 $\mu\Omega\cdot$cm at 3 K. The resistivity reaches the value of 25.0 $\mu\Omega\cdot$cm at 300 K with a linear behavior as a function of temperature in the temperature range from 3 to 300 K, which is classical for a rather good metal. The compound is found to be paramagnetic above 3.5 K, with an effective moment of 1.36 μ_B/unit (or 0.34 μ_B considering one Sm atom) and a Weiss temperature of −17 K, denoting a slight antiferromagnetic ordering. The low value of the experimental magnetic moment compared with the computed value (close to 6 μ_B/Sm) is expected from the large cancellation of the spin moment by the orbital contribution, as reported for $PuCoGa_5$.[42] As pointed out in a previous study of the ternary phase $Sm_2Co_{17-x}Ga_x$ ($x = 0-7$),[43] the Ga substitution for Co leads to an approximately linear decrease in the Curie temperature and a rapid decrease in the saturation magnetic moment, which is faster than that in the case of magnetic dilution. Therefore, the absence of ferromagnetism in the compounds studied, which are rich in Ga, is not surprising.

From magnetic and electrical measurements, we show the evidence for bulk superconductivity in $Sm_4Co_3Ga_{16}$. A transition to zero resistance is observed near 2.8 K (Figure 10); this value is almost co-incident with the shielding diamagnetism observed at 3.2 K (Figure 11). The full-shielding diamagnetism is not observed, certainly in relation with the presence of paramagnetic impurities in the bulk sample. The discrepancy between these two values is due to a slight offset of the temperature probe in the VSM cryostat. This temperature is very close to the value of 2.3 K found

---

(42) Opahle, I.; Oppeneer, P. M. *Phys. Rev. Lett.* **2003**, *90*, 157001.
(43) Liang, B.; Kleinschroth, I.; Shen, B.; Kronmuller, G., H. *J. Appl. Phys.* **2000**, *87*, 5314.

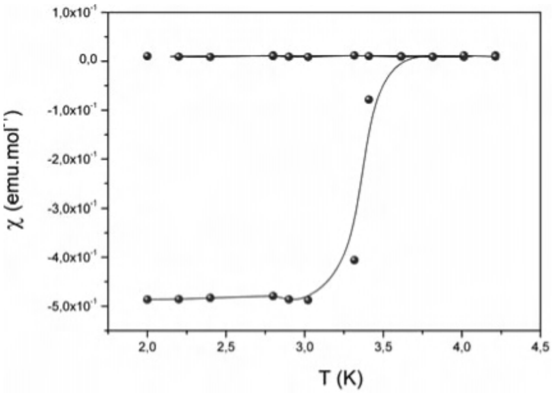

Figure 11. ZFC/FC magnetic susceptibility measurements for compound $Sm_4Co_3Ga_{16}$ (ac mode).

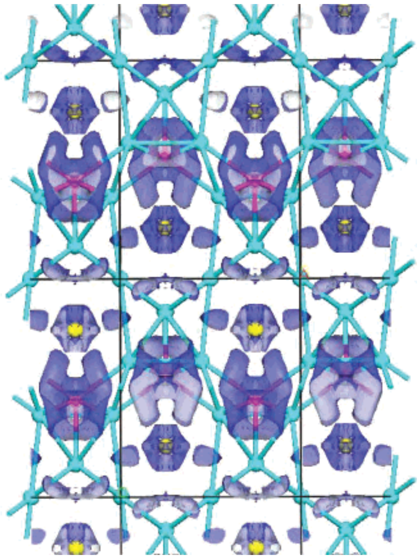

Figure 12. Representation of the electron-density difference (isovalue level 0.021 e·Å^{-3}) calculated for $SmCoGa_4$.

for the HF $CeCoIn_5$ compound, which displays a resistivity of 8 $\mu\Omega$·cm at 3 K. The studies on the superconductivity of $PuCoGa_5$ have suggested the occurrence of unconventional superconductivity. In such a scenario, the order-of-magnitude-lower T_c value for $Sm_4Co_3Ga_{16}$ as compared with that of $PuCoGa_5$ ($T_c = 18.5$ K) would result from a decrease in the bandwidth in going from 5f to 4f electrons that have a greater degree of localization. In the case of $Sm_4Co_3Ga_{16}$, superconductivity should almost exclusively be driven by lattice-vibration pairing.

$SmCoGa_4$. The assumption that in these compounds Sm bears a 3+ formal charge in agreement with its lowest electronegativity is supported not only by the DFT calculation but also by the magnetic measurements carried out for $Sm_4Co_3Ga_{16}$. This is very well illustrated in the electron-density difference map (Figure 12) calculated for $SmCoGa_4$ in which the Sm atom bears a 2.678+ charge and in which the main bonding involves the Co and Ga1 atoms (see Figure 6 for atom labeling). With regard to the Mulliken atomic charges (Table 10), the structure can be roughly divided into two anionic domains, the corrugated Co/Ga1 layer with a mean atomic charge of 0.236− and the 2D square network (mean atomic charge of 0.533−) in which the bonding is weaker (Ga2−Ga3: 2.8765 Å). The electron-density difference map also gives evidence of the strong polarization that the Sm cation exerts on bonds forming the 17-vertex cage in which it is lying.

Concluding Remarks

In this paper, we have reported the existence of three novel compounds in the ternary system Sm−Co−Ga. $SmCoGa_5$ (**I**) displays the same tetragonal structure as $PuCoGa_5$ and $Sm_4Co_3Ga_{16}$ (**II**) is strongly related to the $SmCoGa_5$ structure, although the orthorhombic compound $SmCoGa_4$ (**III**), of the $YNiAl_4$ type, is quite different. The common feature of these compounds is that they are built from the stacking of atomic layers: plane SmGa and crown-$CoGa_4$ for **I** and plane $CoGa_4$, quasi-plane SmGa, and crown-$CoGa_4$ for **II**. The structure of **III** is composed of corrugated layers of Ga, layers of Sm, and corrugated layers of $CoGa_2$. $SmCoGa_5$ and $PuCoGa_5$ have the same tetragonal structure as the quasi-2D HF $CeCoIn_5$ compound that displays a superconducting transition at 2.3 K. The properties of the latter have been discussed in consideration of the stacking along the 4-fold axis of monolayers of the face-sharing distorted cuboctahedra $CeIn_3$ and the monolayers of edge-sharing rectangular parallelepipeds $CoIn_2$.[44] In addition to their electronic descriptions, the origin and level of superconduction in these systems may be correlated with their geometrical features, as for the $CeMIn_5$ series.[44]

With the most distorted cuboctahedra, $CeCoIn_5$ and $CeIrIn_5$ exhibit ambient pressure superconductivity below 2.3 and 0.4 K, respectively, whereas $CeRhIn_5$, in which the $CeIn_3$ cuboctahedron is the most regular, is antiferromagnetic at ambient pressure with $T_N = 3.8$ K, like the cubic $CeIn_3$ ($T_N = 10$ K). Interestingly, superconductivity can be induced in the latter at a very low T_c (below 200 mK) by applying a pressure of 2.5 GPa. Now, the comparison with $PuCoGa_5$ is worthy because in this compound Pu is located at the center of a very regular cuboctahedron (quasi-perfect $m\bar{3}m$ symmetry). The superconductivity in $PuCoGa_5$, which experiences a T_c of 18.5 K (22 K at 16.4 GPa),[2] arises from a pairing mechanism either mediated by lattice vibrations with electron pairs having no relative angular momentum (isotropic *s*-wave) or magnetically mediated (p or d wave), as is the case for HF materials and high T_c superconductors.

In $SmCoGa_5$, the distortion of the $SmGa_3$ cuboctahedron is roughly similar to that found for the $CeIn_3$ cuboctahedra in $CeCoIn_5$ and $CeIrIn_5$, suggesting possible superconducting properties that have not been investigated because $SmCoGa_5$ could not be obtained as a pure phase.

However, the study of these new ternary compounds seems promising if one considers the evidence for superconductivity in the $Sm_4Co_3Ga_{16}$ compound. Indeed, the close relationship between the distortion in the local environment of the f elements (Pu in the case of $PuCoGa_5$) and the value of the critical temperature observed for the actinide-based com-

---

(44) Moshopoulou, E. G.; Sarrao, J. L.; Pagliuso, P. G.; Moreno, N. O.; Thompson, J. D.; Fisk, Z.; Ibberson, R. M. *Appl. Phys. A* **2002**, *74* (*suppl. 1*), S895.

pounds was qualitatively corroborated by our results. The T_c measured on our $Sm_4Co_3Ga_{16}$ sample (∼3 K), albeit low compared with any technological requirement, could be varied by considering other parameters like stoichiometry and pressure. Furthermore, this family is based on nonradioactive elements, which allow a comprehensive study without protracted precautions and without any temporal evolution of the compounds.

Supporting Information Available: One CIF file. This material is available free of charge via the Internet at http://pubs.acs.org.

IC0700755